Phosphorescence Mechanisms. II. Description of Phosphorometer

C. BILLINGTON
Commonwealth Scientific and Industrial Research Organization, Division of Chemical Physics, Chemical Research Laboratories, Melbourne, Australia

(Received June 13, 1960)

The functions of the phosphorometer are (i) to excite the phosphor under test with ultraviolet radiation whose intensity is modulated sinusoidally, (ii) to measure the modulation frequency, and (iii) to sample the excitation and emission intensities, and to extract from their modulated components the in-phase attenuation factor between them. The Hg arc source is current-modulated and stabilized by optical feedback over the range 3 to 30 000 cps. The average intensity of both excitation and emission is used to control the sensitivity of their respective photodetectors so that the modulation signals are always referred to the same datum. Both signals are passed in turn through a homodyne detector whose phase is adjusted to identity with the excitation modulation. The in-phase attenuation factor which is the ratio of the homodyne outputs is determined potentiometrically with a probable error of about 0.002.

THE OPTICAL SYSTEM

THE optical system is set out diagrammatically in Fig. 1. The arc chosen was the strongest source of 3650-A radiation readily available. The field lens focusses the arc electrodes on the condenser lens. The stop provides a definite circle of even illumination on the phosphor holder. The filter $F1$ is a Wratten 18A glass filter which transmits only the 3650-A group. The glass slide deflects about 8% of the whole cone of exciting radiation onto a vacuum photocell whose output is used for monitoring both the average brightness, and the waveform and depth of modulation. A visual inspection of the phosphor and the optical line-up is possible by viewing from the opposite side of the glass slide. The phosphor powder is stuck to its copper holder with a minimum of collodion dissolved in alcohol. The Dewar vessel which has a transparent base is evacuated after assembly, and the temperature of the phosphor is closely that of the liquid in the flask. By this means temperatures between liquid air and boiling water are attainable, though adequate stirring and control involve complications.

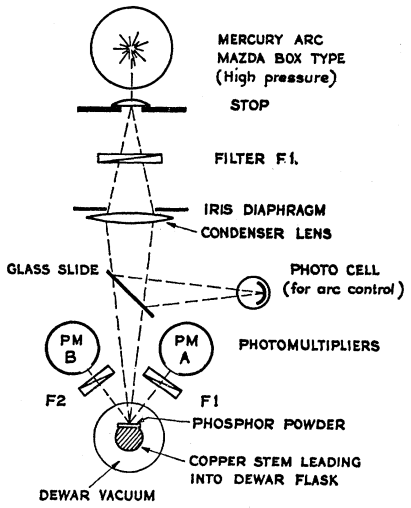

FIG. 1. Arrangement of the optical components of the phosphorometer.

Since it was desired to use opaque phosphors in powdered form the emission had to be sampled from the front surface, which fixes the position of the photomultiplier PM B. The filter $F2$ is ideally complementary to $F1$, and the Wratten type $2A$ is fairly satisfactory. The excitation sampling photomultiplier in position PM A receives scattered uv radiation from the phosphor and requires another filter $F1$. With this photomultiplier in an alternative position equivalent to that of the photocell, slight errors appeared in the measured depth of modulation. This was presumed to be due to the variable sensitivity across the photocathode combined with residual nonuniformities of depth of modulation across the field stop.

Due mainly to slight fluorescence of $F2$ a fraction of the exciting illumination reaches PM B. This amount is not a function of the luminous efficiency of the phosphor, and for the efficient phosphors which have been studied to date it is negligible compared with the emission intensity. For less efficient phosphors this "straight through" signal will not be negligible, and will appear in the phosphorogram as a concurrent component of very high rate constant. This sets an effective lower limit to the efficiency of phosphors which are suitable for measurement.

In order to obtain a two-dimensional optical bench, the several subassemblies of Fig. 1 are mounted at the appropriate height on the closed ends of loudspeaker magnets. The open ends of the magnets are ground flat, and the assemblies mounted firmly on a roughly ground and flat $\frac{5}{16}$-in. steel base plate. The magnetic force and friction is strong enough to resist vibration or an accidental knock, but at the same time allows sensitive adjustment of position at a definite height above the base plate.

THE OSCILLATOR

The stability of the oscillator which is used as the primary source of optical modulation has to be higher than that normally available in a commercial unit. An

RC oscillator is suitable for the wide frequency range, having good waveform and more than adequate frequency stability. However most commerical oscillators exhibit amplitude instabilities greater than 0.1%. The oscillator used was a Model *M2 RC* Oscillator by Southwestern Industrial Electronics, which was found to possess amplitude stability at least as good as 0.01%. Frequency measurement was accomplished by simultaneously counting cycles from the oscillator and from a standard 1000-cps tone for a period long enough to provide an accuracy exceeding 0.1%.

MODULATION AND STABILITY OF THE ARC

Mechanical modulation of the light source is not suitable because of the purity of the waveform and the range of modulation frequency that are needed. An ultrasonic cell modulator was tried in the initial stages but it was found to be too wasteful of light, and was abandoned in favor of direct modulation of the arc current. The arc operates at an almost fixed voltage in conjunction with a ballast resistor from a stabilized supply. Shunt tubes carrying an average current of about $1\frac{1}{2}$ amp allow current modulation of the arc by a voltage signal applied to their control grids. Mazda type *N*37 tubes were used for this purpose because of their availability, high mutual conductance and current-carrying capacity, and tolerance of low plate voltage without distortion. The arrangement is shown at the top left of Fig. 2. Coupling an oscillator to these parallelled grids with suitable bias provides a modulator of good waveform up to 10% depth of modulation. For frequencies above 1000 cps the efficiency of modulation declines, but the loss of efficiency can be offset by increasing the modulating signal up to about 8000 cps. Too great a modulating signal causes marked instability in the arc and often leads to extinction.

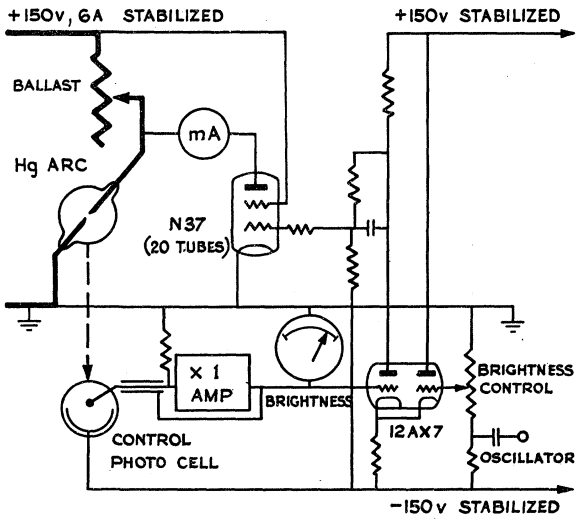

FIG. 2. Simplified circuit diagram of the arc stabilizer and modulator.

Although the supply voltage has a stability of ±0.05%, this simple method lacks adequate stability in the average level of illumination, because of movement of the arc itself. A fivefold improvement in stability was achieved by using a monitor photocell and including the arc in a feedback loop whose arrangement is set out in Fig. 2. The loop is direct-coupled so that small changes of arc brightness caused by movement of the arc are compensated by changing the arc current. Modulation and brightness control are conveniently introduced by using a differential amplifier in the loop. This method has the additional advantage that the brightness and depth of modulation can be adjusted independently, and that the decreasing efficiency of modulation after 1000 cps is automatically compensated. The oscillator output is tailored by a filter (not shown in the figure) to reduce the modulation at high frequencies to a safe level. The arc is operated close to its rated maximum wattage. When a reduced intensity of radiation is required, the iris diaphragm of Fig. 1 is used in conjunction with the brightness control so as to maintain the arc and shunt tubes at the same working points.

PHOTODETECTORS AND DEMODULATOR

The analytical expressions for the excitation and emission intensities and for the in-phase attenuation factor are reproduced here from Part I;

$$I_{\text{exc}}=A\{1+a\cos\omega t\}, \tag{1}$$

$$I_{\text{em}}=B\{1+a\lambda\cos(\omega t+\phi)\}, \tag{2}$$

and

$$\chi=\lambda\cos\phi. \tag{3}$$

Before the modulation parameters a and $a\chi$ can be measured the average intensities of the radiation sampled by the two photodetectors must be referred to the same datum level. For this purpose it is convenient to use photomultiplier tubes because their sensitivity can be voltage-controlled. Photomultiplier, power supply, and integrating filter can be arranged in a closed loop to give ac voltages, $Ka\cos\omega t$ and $Ka\lambda\cos(\omega t+\phi)$, which are independent of the average intensities A and B over a wide range. The arrangement is shown diagrammatically in Fig. 3.

The short shielded leads from the two photomultiplier collectors are connected to a common load at the input to a dc amplifier. This arrangement ensures that the photomultiplier loads are identical although the additional capacitative loading reduces the performance at high modulation frequencies. The desired channel is selected by applying the supply voltage only to the appropriate photomultiplier.

The dc amplifier whose input and output working points are both at zero voltage makes the effective collector supply voltage nearly 100 V, so that sufficient control will be achieved if the average output voltage can be kept within ±0.1 V, i.e., ±0.1%. The integrating filter *RC* (~1 sec) separates this average voltage from the modulation signal. The voltage across the capacitor *C* is the error voltage which is amplified and used to control the over-all dynode voltage applied to the selected photomultiplier

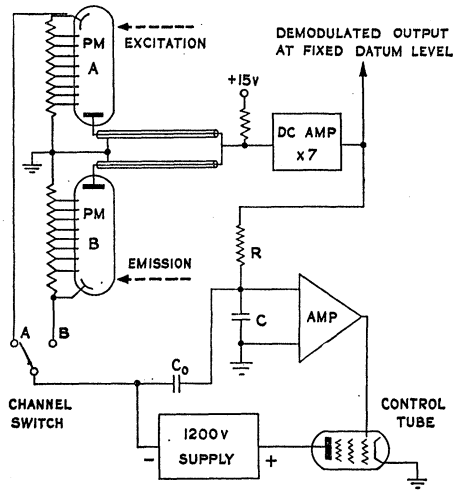

FIG. 3. Schematic diagram of photodetectors and demodulator. The average value of the signal voltage from the selected photomultiplier is constrained to be zero by using it in a feedback loop to control the PM sensitivity.

tube. The E. H. T. supply is not regulated in the usual sense because sustained mains changes are absorbed by the dc loop just described. However ripple voltage which remains after conventional filtering is not passed by the *RC* filter, and so is removed by an auxiliary loop through the capacitor C_0.

The performance of the whole arrangement is adequate for over-all dynode voltages between 300 V and 800 V. A 10% depth of modulation ($a=0.1$) produces an output of about 7 V rms (i.e., $K\cong 70$ V). At very low frequencies a significant proportion of the modulation passes the *RC* filter and enters the control loop. The conversion factor K is therefore not independent of frequency, but linearity is however sufficiently maintained, and the ratio χ is found to be unaffected down to $3\frac{1}{2}$ cps.

THE HOMODYNE DETECTOR

The terminology is in accord with that of Tucker[1] who has carefully studied the communications aspects of the device. It consists of a chopper which effectively multiplies the incoming signal, $Ka\cos\omega t$, by a gating function $G[\cos(\omega t+\zeta)]$ which has the value unity when the argument is positive and zero when it is negative. The product may be shown to be

$$P=(Ka/\pi)\cos\zeta. \tag{4}$$

Applying this to the present case with channel A as the input function, if the phase of the gating function is adjusted so that $\zeta=0$ then the detector output will be

$$P_A=Ka/\pi. \tag{5}$$

If now the phase of the gating function is *not* readjusted for channel B, we have

$$\zeta=-\phi,$$

and

$$P_B=(Ka\lambda/\pi)\cos\phi=Ka\chi/\pi. \tag{6}$$

Combining (5) and (6)

$$\chi=P_B/P_A. \tag{7}$$

[1] D. G. Tucker, J. Brit. Inst. Radio Engrs. **14**, 143 (1954).

Thus the analysis of the homodyne detector is simple and appropriate to the present problem. There are no nonlinearities at low input levels. Noise in the input is not rectified by the detector and can be greatly reduced by output filtering. Even harmonics are rejected, and the third harmonic which is almost negligible in the input is further reduced by a factor of three.

Realization of such a strictly quantitative form of the homodyne detector involves precision electronic hardware of a type which does appear to have been previously described. The account given in the following paragraphs is intended as an indication of how the claimed performance was achieved, but not as a complete technical description. A flow diagram for the whole apparatus is given in Fig. 4.

The Gate

The strict linearity requirements exclude the use of diodes, but can be met by a gate consisting of a pair of cathode followers with their cathodes coupled. A diagram of the arrangement and the associated waveforms are shown in Fig. 5.

The gating signal is fed to one grid, and the input signal to the other. If the cathode follower tubes are of the sharp-cutoff type the ratio of gain between either grid and cathode can exceed 70 db if the grids are separated by about 5 V. Thus the gate will be satisfactorily closed if the gating signal is maintained at least 5 V more positive than the peak value of the input signal. Because of the cathode follower action the gain will be closely linear in the open condition provided the gating voltage is kept more than 5 V below the negative peak value of the input voltage. It will be seen that as the positive part of the gating signal contributes to the average value of the output, the positive level must be closely controlled, but the negative level need only be sufficiently negative.

The required gating signal is unfortunately rather large, and at least half of it inevitably appears as "ripple" at the output. In order to achieve 0.1% resolution with A channel signals of about

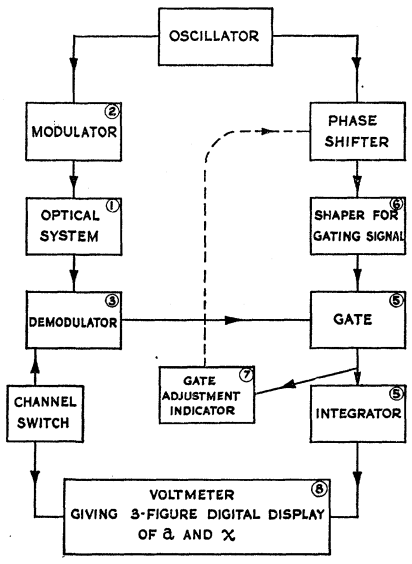

FIG. 4. Block diagram of phosphorometer.

7 V rms, changes of about 3 mv dc in the average level of the output have to be detectable in the presence of an ac signal of nearly 20 V peak-to-peak. At low frequencies this is very difficult to attenuate sufficiently, and requires several stages of *RC* integration. Capacitors with low soakage have to be used. A quick charging arrangement is convenient to reduce the time taken to reach equilibrium.

For normal optical intensities this filter is more than sufficient to cope with the optical noise, and it is the slow components of instability throughout the system which are the final limitation to the accuracy attainable. The filter also determines the low-frequency limit of the apparatus. It is found that below about $3\frac{1}{2}$ cps, voltmeter readings are impracticable. Increase in the number of *RC* stages or in their time constant would only increase the time taken for a complete set of readings, and so impose more stringent stability requirements over the whole apparatus.

The Gating Signal

Some of the requirements for the gating signal are implied by the previous section, and some by the mathematical treatment. They are the following:

(i) The waveform must be rectangular, and the amplitude at least ± 15 V with respect to ground.

(ii) The average value of the positive level must be constant to better than 3 mv, i.e., 0.05%, and independent of frequency.

(iii) The open time of the gate must not differ from the closed time by as much as 0.1% throughout the frequency range; this corresponds to the positive part of the gating signal having a phase duration of $180° \pm 0.2°$.

The waveform is made rectangular by regenerative amplification. Two stages are required to give rise times of about 0.5 μsec and closely flat tops. A suitable type of regenerative stage is illustrated on the right of Fig. 6, in which the anode-to-grid couplings are shown only diagrammatically.

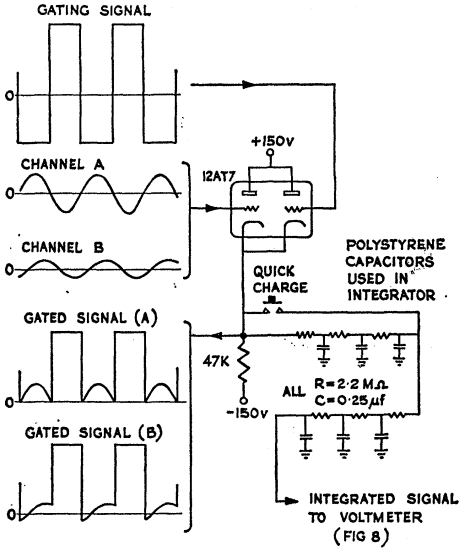

FIG. 5. Gate and integrator, showing also the input and output waveforms on the left. Only half of each cycle from the demodulator is passed to the dc voltmeter. The phase of the gating signal is adjusted to be symmetrical with respect to the channel *A* signal.

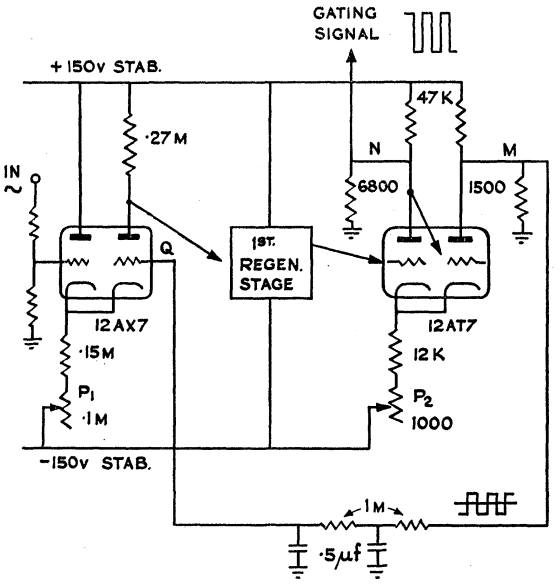

FIG. 6. Schematic diagram of an arrangement for providing a gating signal of precisely half a cycle duration from a sine wave input.

The level and stability of the positive excursions of the anodes of the last stage are dependent only upon two resistors and the positive supply which is stabilized to better than 0.02%. The voltage at the anode *N* which swings between 22 V and -16 V is a suitable signal to drive the gate. The negative excursion of the anode *M* is adjusted statically to be equal and opposite to its positive excursion by means of the cathode resistor *P*2, so that now the mean value of the voltage at *M* is proportional to the differential phase duration between the two stable modes. This mean voltage is developed at *Q* by the integrating network shown in the lower part of Fig. 6. With the smallest sinusoidal input signal which ensures regenerative action, the variable resistance *P*1 is adjusted so that the voltage at *Q* is zero. The 100% dc negative feedback maintains this output condition subject only to unamplified dc drifts associated with the input stage.

The positive excursion at *M* is about 5 V, and with heater stabilization the negative excursion can be kept within 0.05%, which corresponds to a phase differential of less than 0.1°. The less stable negative excursion of *N* does not affect the operation of the gate. The mean voltage at *M* is found to remain within ± 2 mv for frequencies between 3 and 7000 cps, and thereafter to rise steadily to 20 mv at 40 kcps. At these higher frequencies the departure of the waveform from a true rectangle becomes noticeable also.

Hysteresis in the regenerative stage is inevitable if the rise time is to be adequate. It causes a phase shift between the sine wave input and the rectangular wave output which is dependent upon the input amplitude but almost independent of frequency. This has two complicating effects. (i) Because this frequency-independent phase shift cannot be easily compensated automatically, a manually adjustable phase shifter (and with it an out-of-phase detector) must be included and adjusted at each change of frequency. (ii) The sinusoidal output voltage of the phase shifter must be independent of the shift it introduces. An adequate phase shifter has already been described by the author.[2]

PHASE ADJUSTMENT

The nature of the detector output voltage (4) shows that it is insensitive to small phase adjustments in the

[2] C. Billington, Electronic Eng. **30**, 480 (1958).

region $\zeta=0$, which is the condition for measurement of the "A" channel signal; but this is not necessarily true in the case of the "B" channel where $\zeta(=-\phi)$ may be appreciable. Accordingly it is necessary to set ζ precisely for accurate measurement of the quantity $Ka\chi$, and this cannot be done adequately by maximizing the output from the "A" channel signal.

A more sensitive adjustment of ζ can be made from displaying the waveform titled "Gated Signal (A)" of Fig. 5 on an oscilloscope, and adjusting for a symmetrical pattern. The conditions are improved by expanding the trace vertically and examining only the relative depths of the sharp points of the waveform which represent the beginning and end of the open part of the gate. When these two depths are equal, ζ vanishes. In practice ζ can easily be reduced to within a fraction of a degree from zero with a sophisticated oscilloscope, and the limit is set by noise appearing at the sharp points.

A less fatiguing and cheaper method was developed from this and is shown in Fig. 7. The principle is essentially that of a slide-back voltmeter whose cutoff voltage is fixed close to the average voltage of the two negative extremes of the gated waveform, and which accepts only more negative voltages. It will be seen that unbalance at either side of $\zeta=0$ increases the current through the meter, and that by minimizing the meter reading ζ can be made very small. A silicon diode is necessary to give sufficient back resistance. In the practical circuit, cathode followers are used to isolate the diode from the gated signal. On the right of the figure the sensitivity characteristics are sketched for three values of the bucking voltage. The noise which limited the oscilloscope method appears here as a dc displacement of the minimum meter reading.

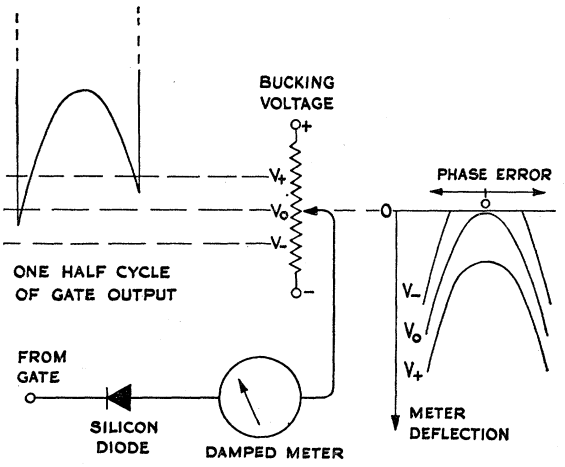

FIG. 7. Visual method of detecting phase displacement of the gating signal with respect to the channel A sine wave. The phase is adjusted manually for minimum meter deflection. On the right is a diagram of the null-sensitivity characteristics for representative bucking voltages V_-, V_0, V_+.

DISPLAY AND OPERATING SEQUENCE

Following the gate and integrator a potentiometric voltmeter is used since 3 decimal places are required for the measured voltages. The potentiometer affords storage facilities which are used both to remove zero offset, and to do the division (P_B/P_A) internally. As shown in Fig. 8 a single servo-amplifier balances in turn three motor-driven helical potentiometers with appropriate inputs selected by the channel switch (see also Fig. 4). The shafts of two of the potentiometers are coupled to 3-figure registers which provide a digital readout. By appropriate adjustment of scale factor the "a" register may be made to indicate the depth of modulation directly. The slow speed of response is no disadvantage in view of the very long stabilizing time of the integrator (~20 sec).

The operating sequence is as follows. With the channel switch at "Z" which automatically grounds the gate input, the oscillator is adjusted to approximately the

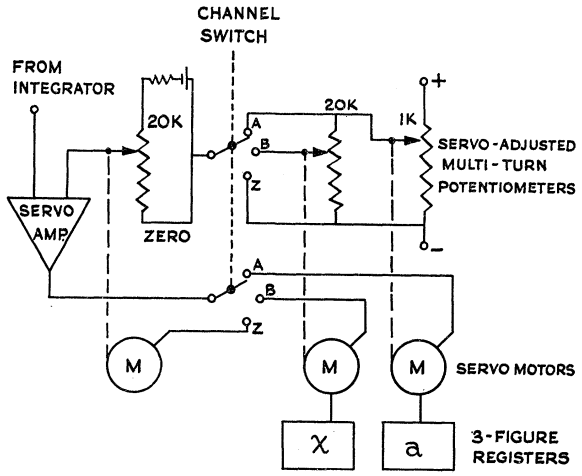

FIG. 8. Potentiometric voltmeter giving direct digital display of the depth of modulation a and the in-phase attenuation factor χ.

desired frequency, and the frequency meter is set counting. When the zero potentiometer is balanced, the channel switch is set to "A" and the phase-shifter adjusted manually. At balance the register gives the value of the depth of modulation a, and the potentiometer establishes the appropriate scale expansion for the potentiometer associated with channel B. The channel switch is then set to "B", and on balance the ratio P_B/P_A (7) appears directly on the other register. This value of χ and the measured frequency are recorded, and are represented by a single point on the phosphorogram. Ordinarily points are measured at equal logarithmic intervals of frequency at the rate of about ten to the decade.

TESTING AND PERFORMANCE

Since no phosphor material is positively known to have a simple mechanism which can be completely

defined by a single rate constant, it is not possible to check the performance of the whole apparatus by means of a test run. A trivial exception is that of very short-lived phosphors which can be used to check the relation $\chi=1$ at all measurable frequencies.

The constancy of the dc output of the demodulator can be simply checked, and this verifies the proper adjustment of the modulation reference level.

The part of the apparatus following the demodulator is not affected by the origins of the electrical signals it receives provided they are coherent, so this part can be tested by substituting a dummy electrical "phosphor" for the optical part of the phosphorometer as shown in Fig. 9. Phosphorograms were run for dummy phosphors of three different rate constants so as to cover nearly

TABLE I. Test results for dummy phosphors.

Test No.	Frequency range cps	No. of points	Rate constant	RMS difference	>0.004[a]	>0.006[b]
1	4 to 300	28	151	0.00181	1	0
2	18 to 1800	39	1380	0.00252	3	0
3	170 to 18 000	33	13 700	0.00262	4	1

[a] Number of points with difference greater than 0.004.
[b] Number of points with difference greater than 0.006.

all the usable frequency spectrum of the apparatus. The three sets were analyzed by plotting the phosphorograms on an extended scale together with a calculated phosphorogram defined by a single rate constant of approximately the same magnitude. To refine the value of this guessed rate constant, the horizontal differences ($\Delta \log f$) between the two plots were summed, and the rate adjusted to make this sum vanish. For this operation only points on the steeper part of the phosphorogram ($0.9>\chi>0.1$) were used. The root mean square of the vertical differences ($\Delta\chi$) from the refined calculated phosphorograms were then computed. A summary is given in Table I.

The three sets of data can be used together to test any frequency-independent error by plotting all the vertical differences against register indication. Such an

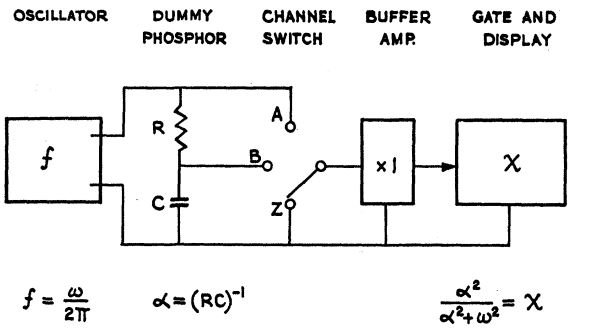

FIG. 9. The arrangement of an electrical filter RC as a "dummy phosphor" for checking the performance of the electronics and display.

error was observable from this plot but it amounted to less than 0.002 for all values of χ. Deducing a reasonable correction curve from this plot and applying it to the same points, the rms difference for all points together can be reduced from 0.0024 to 0.0021. Values of χ for which there were the largest differences between the three sets appeared to be randomly distributed. These calculations take into account all the measured points. It is however more realistic to discard some 8 points out of the 100 because they appear from an initial plot to be incompatible with their neighbors: all but one of these correspond with the 8 points of large difference listed in Table I. If these were discarded the rms difference falls to 0.0019 for all sets together, and to 0.0015 if the correction curve is applied in addition.

CONCLUSION

The tests on dummy phosphors with the phosphorometer described suggest that the probable error in making measurements of the variable is independent of its value and almost independent of frequency within the accessible range. The value of the rms difference ($\Delta\chi=0.002$) sets a standard for the goodness of fit to be achieved in analysis of phosphorograms which is the subject of Part III.